JOURNAL OF Applied Polymer SCIENCE

POSS Core Star-Shape Molecular Hybrid Materials: Effect of the Chain Length and POSS Content on Dielectric Properties

Fuyou Ke,[1] Chao Zhang,[1] Shanyi Guang,[2] Hongyao Xu[1]

[1]Department of Polymer Science and Engineering, College of Material Science and Engineering, and State Key Laboratory of Chemical Fibers and Polymeric Materials, Donghua University, Shanghai 201620, China

[2]Department of Basic Chemistry, College of Chemistry and Chemical Engineering, Donghua University, Shanghai 201620, China

Correspondence to: H. Xu (E-mail: Hongyaoxu@163.com)

ABSTRACT: A series of inorganic–organic molecular hybrids, poly(styrene-*co*-octavinyl-polyhedral oligomeric silsesquioxane)s (PS-POSSs), were synthesized, and their structures and properties were characterized by FTIR, ^{1}H-NMR, ^{29}Si-NMR, XRD, optical microscopy (OM), and atomic force microscopy (AFM). The chemical incorporation of POSS into polymer matrixes achieves uniform dispersion and makes the resultant hybrids display good film formability. The relationship between molecular structure of these hybrids and their dielectric constants and formation mechanism of low dielectric constant were investigated. The low dielectric constant of the hybrids mainly originates from the increase of free volume, involving the free volume of intrinsic porosity from POSS and an increase in the free volume owing to steric hindrance of bulky POSS. The latter plays a dominant role to increase the free volume and formation of low dielectric constant. Simultaneously, the polymer arm-length has an important influence on the dielectric constant of the star-type hybrids. © 2012 Wiley Periodicals, Inc. J. Appl. Polym. Sci. 000: 000–000, 2012

KEYWORDS: nanocomposites; structure–property relations; dielectric properties; POSS; chain length

Received 8 December 2011; accepted 12 February 2012; published online
DOI: 10.1002/app.37507

INTRODUCTION

With the rapid development of the ultra large-scale integrated circuit technology in microelectronic industry, the continuous miniaturization of device size inevitably brings the increase of resistance capacitance time delay, cross-talks and power dissipation. To resolve the above problems, low dielectric constant materials were urgently demanded to be used as interwire and interlayer insulators,[1–5] which should also possess excellent mechanical and thermal properties, good processability.

Traditional inorganic or organic materials are hard to satisfy all the above requirements. Thus organic–inorganic nanocomposites have been developed in the past decades,[6] including silica/polyimide (PI),[7,8] clay/PI,[9] and clay/PMMA.[10] In particular, the molecular hybrids based on polyhedral oligomeric silsesquioxanes (POSS) have attracted much more attention,[11] because POSS has well defined nanometer-sized cube-like structures with porous inorganic core surrounded by eight organic corner groups (active or inert), and can effectively overcome the difficulty to disperse the particles into organic/polymer matrix uniformly via covalent bonding. Many POSS-based hybrid polymers with different architecture, such as dumbbell-type,[12] pendent-type,[13–16] bead-type,[17,18] star-type[19] or network-type,[20–23] have been prepared and exhibits a number of desirable properties, especially the high thermal stability, good mechanical properties, and low dielectric constant.[24–28] Recently, our group prepared a series of network-like POSS-containing hybrids with flexible organic linking chains between POSS cages via hydrosilylative addition reaction between octahydrido-POSS and diene.[29] After calcinations, the dielectric constant can be further reduced to 1.95.[30] However, the mechanism of dielectric constant variation related to the molecular structures, so far, has not been fully understood.

Many systematic works have been done in our group. It is found that star-type POSS-based hybrids show the lower dielectric constants than pendent-type with the same POSS content owing to the larger free volume in the materials.[31] As the methylene number of flexible organic linking chains in network-like POSS-containing hybrids increased from 2 to 8, the dielectric constant of the hybrid film decreased from 2.78 to 2.43.[29] Seckin et al. also synthesized a series of POSS core star polyimides and investigated the effect of chemical structure of polyimide on the dielectric properties.[19] However, the effect of polymer chain length on the dielectric properties in star-type

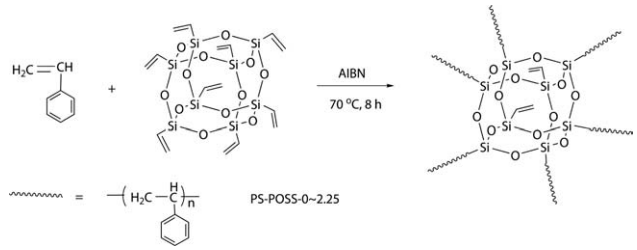

Scheme 1. Formation of star-type POSS-based hybrid nanocomposites.

POSS-based hybrids was not studied. Moreover, the combined effect of how the POSS content and polymer chain length influences the dielectric properties and which is the dominant factor have not been clarified.

To further explore the influence of molecular structure on dielectric constants, in the work, a series of star-type poly(styrene-*co*-octavinyl-polyhedral oligomeric silsesquioxane)s (PS-POSSs) inorganic–organic hybrid nanocomposites were prepared by free-radical polymerization. The relationship between molecular structure and their low dielectric properties, especially the effect of polymer chain length, as well as the forming mechanism of low dielectric constant were investigated in detail.

EXPERIMENTAL

Materials

Octavinyl-polyhedral oligomeric silsesquioxane (POSS) monomer was purchased from Aldrich. Styrene was purchased from Shanghai Reagent, China. AIBN was refined in heated ethanol and kept in a dried box. Spectroscopy-grade THF and 1,4-dioxane were dried over 4 Å molecular sieves and distilled from sodium benzophenone ketyl immediately prior to use. All other solvents were used without further purification.

Synthesis of PS-POSSs

PS-POSSs were prepared via one-step free-radical polymerization technique, as shown in Scheme 1. Taking PS-POSS$_{2.25}$ as an example, the product was prepared as follows: 24.20 mmol (2.520 g) of styrene and 0.80 mmol (0.506 g) of POSS monomer in 20 mL of dried 1,4-dioxane were added in a three-necked flask and stirred for 8 h at 70°C under a nitrogen atmosphere, with AIBN as the initiator (1 wt % on the basis of monomer). The crude product was added dropwise into excess ethanol at 60°C under vigorously agitation to dissolve the unreacted monomers and precipitate the nanocomposite. The product was redissolved in THF to form a homogeneous and transparent solution, and then precipitated in ethanol. This purification procedure was repeated twice to ensure thorough removal of the POSS and styrene from PS-POSS nanocomposite, and finally the product was dried in a vacuum oven. A 36.5% yield was obtained through this procedure.

PS: White powder. M_w = 32700, PDI, 1.83, (GPC, polystyrene). Yield: 46.4%. IR (KBr), υ (cm^{-1}): 699,753 (Ar—C), 1460,1500,1600 (C=C of Ar ring), 2940, 2870 (CH—CH_2). ^{1}H-NMR (500 MHz, $CDCl_3$), δ (TMS, ppm): 1.43 (CH—C*H*$_2$), 1.86 (C*H*—CH_2), 7.26–6.32 (Ar—H).

PS-POSS$_{0.18}$: M_w = 48600, PDI, 1.66, (GPC, polystyrene). Yield: 42.8%. IR (KBr), υ (cm^{-1}): 699,753 (Ar—C), 1109 (Si—O—Si), 1460, 1500, 1600 (C—C of Ar ring), 2940, 2870 (CH—CH_2). ^{1}H-NMR (500 MHz, $CDCl_3$), δ (TMS, ppm): 1.43 (CH—C*H*$_2$), 1.86 (C*H*—CH_2), ~ 6 (Si—CH=*CH*$_2$), 7.26–6.32 (Ar—H). ^{29}Si-NMR (79.49 MHz; solid), δ (ppm): −65.5 (s, *Si*—CHCH$_2$), −79.8 (s, *Si*—CH=CH$_2$).

PS-POSS$_{0.42}$: M_w = 35,200, PDI, 1.69, (GPC, polystyrene). Yield: 40.3%. IR (KBr), υ (cm^{-1}): 699,753 (Ar—C), 1109 (Si—O—Si), 1460, 1500, 1600 (C=C of Ar ring), 2940, 2870 (CH—CH_2). ^{1}H-NMR (500 MHz, $CDCl_3$), δ (TMS, ppm): 1.43 (CH—C*H*$_2$), 1.86 (C*H*—CH_2), ~ 6 (Si—CH=*CH*$_2$), 7.26–6.32 (Ar—H). ^{29}Si-NMR (79.49 MHz; solid), δ (ppm): −65.5 (s, *Si*—CHCH$_2$), −79.8 (s, *Si*—CH=CH$_2$).

PS-POSS$_{1.35}$: M_w = 28,900, PDI, 1.57, (GPC, polystyrene). Yield: 39.6%. IR (KBr), υ (cm^{-1}): 699,753 (Ar—C), 1109 (Si—O—Si), 1460, 1500, 1600 (C=C of Ar ring), 2940, 2870 (CH—CH_2). ^{1}H-NMR (500 MHz, $CDCl_3$), δ (TMS, ppm): 1.43 (CH—C*H*$_2$), 1.86 (C*H*—CH_2), ~ 6 (Si—CH=*CH*$_2$), 7.26–6.32 (Ar—H). ^{29}Si-NMR (79.49 MHz; solid), δ (ppm): −65.5 (s, *Si*—CHCH$_2$), −79.8 (s, *Si*—CH=CH$_2$).

PS-POSS$_{2.25}$: M_w = 17,600, PDI, 1.46, (GPC, polystyrene). Yield: 36.5%. IR (KBr), υ (cm^{-1}): 699,753 (Ar—C), 1109 (Si—O—Si), 1460, 1500, 1600 (C=C of Ar ring), 2940, 2870 (CH—CH_2). ^{1}H-NMR (500 MHz, $CDCl_3$), δ (TMS, ppm): 1.43 (CH—C*H*$_2$), 1.86 (C*H*—CH_2), ~ 6 (Si—CH=*CH*$_2$), 7.26–6.32 (Ar—H). ^{29}Si-NMR (79.49 MHz; solid), δ (ppm): −65.5 (s, *Si*—CHCH$_2$), −79.8 (s, *Si*—CH=CH$_2$).

Characterization

FTIR spectra were measured with a Nicolet NEXUS 870 FTIR spectrophotometer using KBr powder at room temperature. ^{1}H-NMR spectra were recorded on a Bruker DSX-400 spectrometer using chloroform-*d* solvent. High-resolution ^{29}Si-NMR spectra were carried out at room temperature using a Bruker DSX-400 spectrometer operating at resonance frequency of 79.49 MHz. An X-ray diffraction (XRD) study of the sample was carried out with a Bruker AXS D8 Discover instrument with a general area detector diffraction system powder diffractometer and a charged coupling device camera detector (40 kV, 40 mA). The density of octavinyl-POSS was measured with an Ultrapycnometer 1000 automatic gas pycnometer. The solutions of PS-POSS$_{2.25}$ hybrid in THF with 0.1 *M* concentration were spun on Si wafers and dried in room temperature 6 h, then continued for drying under reduced pressure at room temperature for 4 h to form thin films for the investigation of the film formability and the homogeneity. The atomic force microscope (AFM) and optical microscope (OM) images of hybrid films were taken in the tapping mode on a Veeco Nanoscope IV multimode AFM and a CMM-88E metallographic microscope, respectively. The contact-angle measurements of hybrid films were performed by OCA40 Video optical contact angle meter, deionized water and glycerol (99%; Shanghai Reagent) were chosen as the testing liquids. Capacitance measurement was carried out with an Agilent E4980A LCR meter at a frequency of 1 MHz. For capacitance measurement, an array of gold dots ~ 150-nm thick and 2 mm in diameter was deposited on the film surface by

sputtering through a stainless steel mask. Film refractive index (n) and thickness was measured with an ELLIP-SR ellipsometer and fitted with Cauchy model. The dielectric constant (ε_r) of the film was calculated by using eq. (1).[32]

$$\varepsilon_r = C \cdot d/(A \cdot \varepsilon_o) \quad (1)$$

where C is the capacitance of the film; d is the thickness; A is the area of top gold electrode, and ε_o is the permittivity of free space.

Measurements of Increased Relative Porosity

The increased relative porosity (ϕ_r) was determined according to eq. (2):

$$\phi_r = \underbrace{[(d^T - d^M)/d^T] \times 100\%}_{\text{due to increased free volume}} + \underbrace{(0.048 \times V\%)}_{\text{due to the intrinsic pore of POSS}} \quad (2)$$

where d^M is the measured density determined by the division of the weight of the films by their volumes.[14] At least three specimens were used to determine each density data point. d^T is the theoretical density of the POSS-based inorganic–organic hybrid nanocomposites estimated from the weight percentage of POSS in the nanocomposites, where the density of octavinyl-POSS is 1.40 g cm^{-3}, and polystyrene 1.07 g cm^{-3}. $V\%$ is the volume percentage of POSS in the nanocomposites. The nanoporosity core of POSS with a diameter of 0.54 nm in a POSS molecule of 1.5 nm in diameter represents only 4.8 vol % of the total POSS volume as provided by the Hybrid Plastics Co[13]. Thin films of the hybrid nanocomposites were prepared by spin-coating the hybrid solutions (ca. 15 mg mL^{-1}) on silicon wafers.

Determination of POSS Content

IR analysis was used to determine the POSS content of these hybrid materials. The detailed method has been reported in our previous work,[33] and the mole percentage of POSS (Y_{POSS}) in the hybrids can be calculated according to eq. (3):

$$Y_{POSS} = 0.044(I_{1109}/I_{699}) - 0.0094 \quad (3)$$

where I_{1109}, I_{699} being the integral area of characteristic peaks from POSS and organic components in the resulting hybrid nanocomposites.

RESULTS AND DISCUSSION

Structural Characterization of Hybrids

PS-POSSs were prepared with octavinyl-POSS and styrene via one-step free radical polymerization technique. These hybrids were soluble in most of the common organic solvents, such as THF, $CHCl_3$, dioxane, toluene, and so on. The results indicate that the synthesized hybrid nanocomposites are mainly star-type rather than network structure, since network nanocomposites are virtually insoluble in the above solvents.

The structure of PS-POSSs was characterized by the FTIR, ^{1}H-NMR, and ^{29}Si-NMR spectra, and all the hybrids gave satisfactory spectroscopic data corresponding to their expected molecular structures (Figure 1). For instance, the FTIR spectrum of

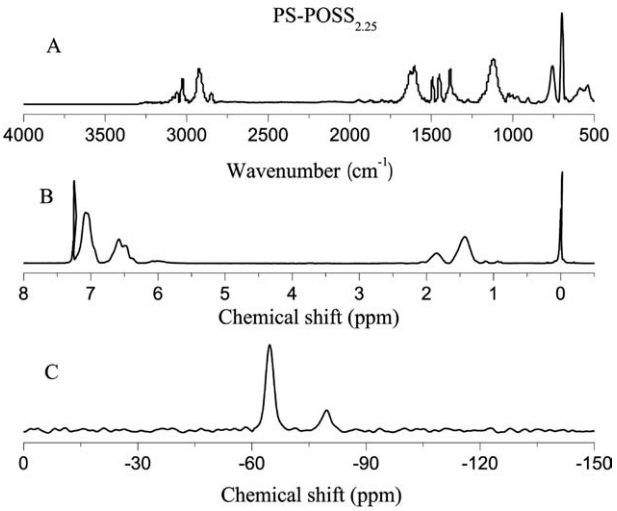

Figure 1. (A) FTIR, (B) ^{1}H-NMR and (C) ^{29}Si-NMR spectra of PS-$POSS_{2.25}$ hybrids.

PS-$POSS_{2.25}$ shows two characteristic out-of-plane wagging absorption bands of single-substituted aromatic ring (699 and 756 cm^{-1}) and a strong symmetric peak of the characteristic Si—O—Si stretching of silsesquioxane cages (1109 cm^{-1}), indicating that the POSS cages are incorporated into the polymeric chains. According to eq. (3), the molar content of POSS can be calculated. The results are shown in Table I. It clearly shows that the molar fraction of POSS in the hybrids increases with the POSS feed ratio, demonstrating that POSS content in the hybrids can be effectively controlled by varying the POSS feed ratio.[33]

The ^{1}H-NMR spectrum exhibits resonance peaks of aromatic ring (7.1 and 6.6 ppm), methine protons (1.8 ppm), and methylene protons (1.4 ppm), respectively. Besides, there is a wide resonance band nearby 6.0 ppm belonging to the unreacted vinyl protons of POSS molecules, suggesting that not all the vinyl groups of POSS have participated in the copolymerization, which is also confirmed by ^{29}Si-NMR spectrum. The ^{29}Si-NMR spectrum shows two resonance bands of the silicon atoms corresponding to the reacted and unreacted vinyl groups on the POSS cages at −65.5 and −79.8 ppm, respectively. Because the peak area at −65.5 ppm is much larger than that at −79.8 ppm, indicating that most vinyl groups of POSS have participated in the copolymerization to form hybrid nanocomposite. By integrating the two peak areas, the average reacted vinyl groups per POSS molecule was calculated as 5.8 in PS-$POSS_{2.25}$ hybrids. In other words, the average number of arms in star-type hybrids is 5.8. The detailed structural characterizations of PS-POSS hybrids have been published in our previous work.[33]

Furthermore, based on the POSS content and the average number of arm in the hybrids, the average polymerization degree of PS chains in each arm [see Table I (U_n)] was calculated. As shown in Table I, the average chain length of each arm decreases with the increase of POSS content. For example, an average polymerization degree of PS chains in each arm of PS-$POSS_{0.18}$ is 70.2, while it is 7.49 in PS-$POSS_{2.25}$. Simultaneously,

Table I. Characteristics of Star-Type POSS-Based Hybrid Nanocomposites

Samples	POSS (mol %) Feed ratio	POSS (mol %) Measured ratio[a]	POSS (vol %)[b]	x[c]	U_n[d]	Dielectric constant (ε_r) (1 MHz)	Refractive index (n)[e] (650 nm)
PS	0.00	0.00	0.00	-	-	2.69	1.630
PS-POSS$_{0.18}$	0.45	0.18	0.83	7.9	70.2	2.61	1.594
PS-POSS$_{0.42}$	0.90	0.42	1.92	7.2	32.9	2.52	1.576
PS-POSS$_{1.35}$	1.60	1.35	5.98	6.7	10.9	2.39	1.533
PS-POSS$_{2.25}$	3.20	2.25	9.67	5.8	7.49	2.32	1.513

[a]Date were obtained based on the IR standard curve, [b]Date were calculated from the weight percentage of POSS in the hybrid nanocomposites and the density of octavinyl-POSS (1.40 g cm^{-3}) and polystyrene (1.07 g cm^{-3}), [c]The average arms in POSS star-type hybrids, calculated on the basis of ^{29}Si-NMR spectrum, [d]The average polymerization degree of PS chains in each arm, calculated according to molar content of POSS and x, [e]Refractive index of the hybrid films were fitted with Cauchy model according to test results of ellipsometer.

the arm number in the hybrids also decreases with the increase of POSS content (from 7.9 to 5.8), indicating that POSS results in low free radical activity of polymeric chain owing to the steric hindrance.[26]

Film Morphology and Homogeneity of the Hybrids

The film formability and dispersity of POSS in the hybrids are crucial for rationally investigating low dielectric properties as well as further applications. All the films were clear and transparent, suggesting that the hybrid films were homogeneous. For further confirming homogeneous film, their optical micrographs images were investigated. Figure 2(A,B) displays the optical micrographs images of PS-POSS$_{2.25}$ at magnification scales 200× and 3200×, in which neither particles nor gas holes were observed, indicating that these hybrids exhibit good film formability. The nanoscale morphology of the hybrid films was further investigated by AFM, as shown in Figure 2(C,D). The surface of the hybrid thin film is quite smooth and has no observable cracks and aggregation of POSS nanoparticles, suggesting that POSS has been uniformly dispersed in the resulting hybrids.

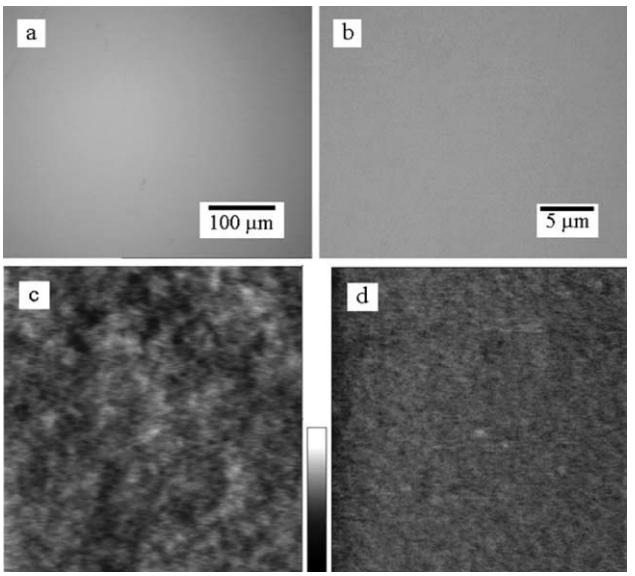

Figure 2. (A) ×200 and (B) ×3200 OM micrographs and 500 × 500 nm^2 tapping mode AFM (C) height and (D) phase images of PS-POSS$_{2.25}$ hybrid film (Z ranges for the height and phase images are 5 nm). [Color figure can be viewed in the online issue, which is available at wileyonlinelibrary.com.]

XRD was also used to characterize the dispersion of POSS in the hybrids. Diffraction patterns of the PS, POSS, and PS-POSS hybrid nanocomposite are shown in Figure 3. The X-ray powder pattern of POSS shows three main characteristic diffraction peaks at 10.7°, 20.9°, and 33.3° (2θ degree). These data are typical for the crystal structure of POSS.[34] A broad amorphous diffraction peak of PS is at about 19.5° (2θ degree). However, in the diffraction patterns of PS-POSS$_{2.25}$ hybrid, only a broad amorphous peak of PS at about 19.0° (2θ degree) is observed. The small shift to smaller angle in the location of the amorphous peak is attributed to POSS molecules propping up polymer chains. The disappearance of POSS crystal peak suggests that no significant aggregation occurs even when the POSS molar percentage is 2.25%, POSS molecules are uniformly distributed in the hybrids. The XRD results indicate that

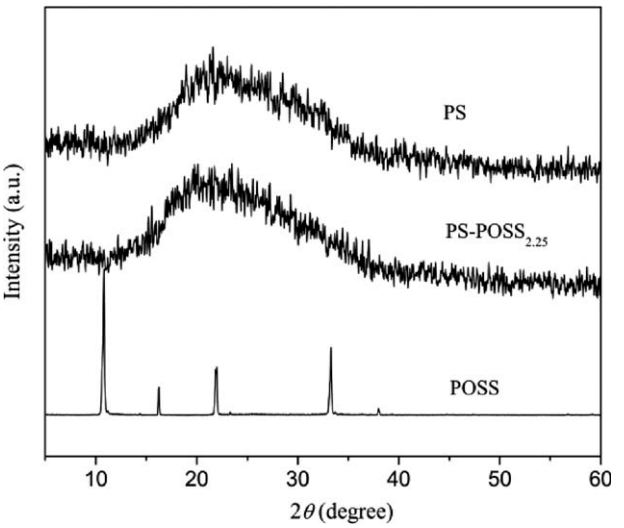

Figure 3. XRD patterns of octavinyl-POSS, PS, and PS-POSS$_{2.25}$ hybrids.

Table II. Physical Properties of PS-POSS Hybrids

Samples	Theoretical density (d^T)[a] (g cm^{-3})	Measured density (d^M) (g cm^{-3})	Rel porosity increase (ϕ_r) (%)	ϕ_r^f (%)[b]	ϕ_r^p (%)[c]
PS	1.070	1.07 ± 0.01	0	0	0
PS-POSS$_{0.18}$	1.073	1.04 ± 0.02	3.22	3.18	0.04
PS-POSS$_{0.42}$	1.076	1.00 ± 0.03	7.04	6.95	0.09
PS-POSS$_{1.35}$	1.091	0.96 ± 0.01	12.3	12.0	0.29
PS-POSS$_{2.25}$	1.108	0.94 ± 0.02	15.2	14.7	0.46

[a]Theoretical density was estimated from the weight percentage of POSS in PS-POSS hybrids, and the density of POSS (1.40 g cm^{-3}) and polystyrene (1.07 g cm^{-3}), [b]Relative porosity increase comes from increased free volume, [c]Relative porosity increase comes from the intrinsic pore of POSS.

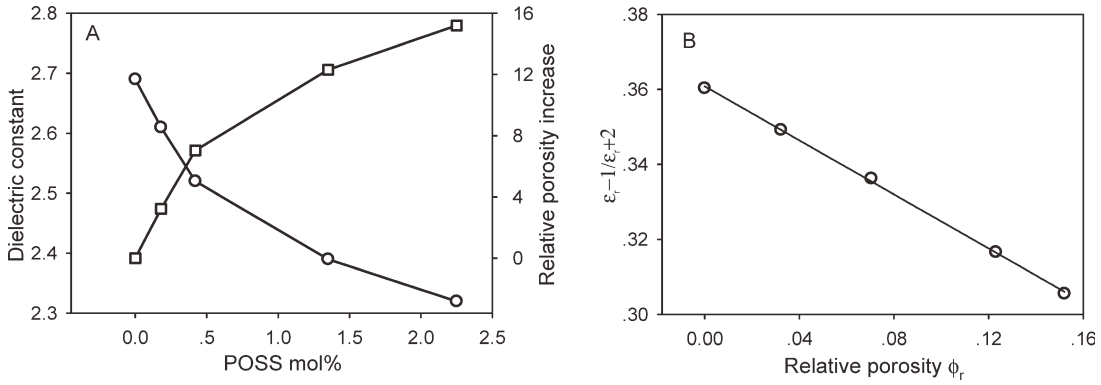

Figure 4. (A) Relationship between the dielectric constant and relative porosity increase for various molar percentages (mol %) of POSS in PS-POSS hybrids; (B) A data fitting according to eq. (4).

incorporation of POSS into polymer matrix via covalent bonding can effectively prevent the self-aggregation of POSS, which is consistent with the results of OM and AFM.

Dielectric Properties of Materials and Forming Mechanism of Low Dielectric Constant

The dielectric constant (ε_r) of PS and the POSS-based hybrids were evaluated by capacitance approach, and their refractive indexes (n) were measured with an ellipsometer and fitted with Cauchy model. The results are summarized in Table I. The dielectric constants of PS-POSS hybrids are all lower than that of PS, demonstrating that incorporation of POSS into polymer matrix can effectively reduce the dielectric constant (ε_r) of the resulting hybrids, which may be attributed to introduction of intrinsic porosity from POSS and an increase in the free volume owing to steric hindrance.[21,35] Thus the dielectric constants of the hybrids decrease with the POSS content, from 2.69 for PS to 2.32 for PS-POSS$_{2.25}$. Simultaneously, it was found that the dielectric constants decrease with the decrease of average PS arm chain length (arm-length, U_n) in star-type PS-POSS hybrids. For instance, when U_n reduces from 70.2 to 7.49, ε_r significantly decreases from 2.69 to 2.32. Similar phenomenon was observed in the measurement of refractive index (n) of PS-POSS hybrids.

To further investigate forming mechanism of the low dielectric constants of PS-POSS hybrids, we quantified the contribution of the increased free volume and the intrinsic pore of POSS to the increased relative porosity (ϕ_r) ($\phi_r = \phi_r^f + \phi_r^p$) based on eq. (2). The results are listed in Table II, where the ϕ_r^f is the increased amount of free volume due to the incorporation of bulky POSS into polymer, ϕ_r^p is the nanoporosity of POSS molecules themselves. ϕ_r^f values are far greater than ϕ_r^p, indicating that the increase of free volume plays the dominant role to the decrease of the dielectric constant in PS-POSS hybrids. Figure 4A shows the relationship between the ε_r and ϕ_r for various POSS contents in PS-POSS hybrids. ϕ_r values of PS-POSS hybrids obviously increase with increase of POSS content, which

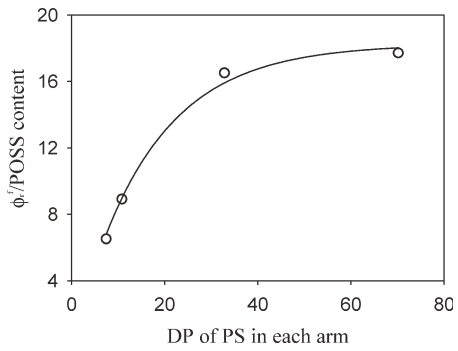

Figure 5. Relationship between the averaged increasing free volume by POSS content and PS arm-length.

Table III. Surface Properties of Star-Type POSS-Based Hybrids

Samples	Θ (°±σ) Water	Θ (°±σ) Glycerol	γ_s (mN m^{-1})[a]	γ_s^d (mN m^{-1})[a]	γ_s^p (mN m^{-1})[a]
PS	73.8 ± 1.3	70.2 ± 0.9	34.6	13.9	20.7
PS-POSS$_{0.18}$	76.5 ± 1.1	72.4 ± 1.2	32.9	13.6	19.4
PS-POSS$_{0.42}$	79.2 ± 0.8	74.3 ± 0.5	31.3	13.5	17.9
PS-POSS$_{1.35}$	84.5 ± 1.4	79.7 ± 1.1	28.1	12.4	15.6
PS-POSS$_{2.25}$	86.7 ± 0.9	81.1 ± 0.7	26.8	12.2	14.6

[a]Calculated with Wu's harmonic mean method.

perfectly corresponds with the decrease of their dielectric constants. It is known that the relationship between the dielectric constant of porous materials (ε_r) and increased relative porosity (ϕ_r) can be expressed as eq. (4).[36]

$$\frac{\varepsilon_r - 1}{\varepsilon_r + 2} = (1 - \phi_r)\frac{\varepsilon_{r0} - 1}{\varepsilon_{r0} + 2} \quad (4)$$

where ε_{r0} is the dielectric constant of the materials without introduced porosity. Thus, a fit according to eq. (4) is applied to these data in Tables I and II, as shown in Figure 4B. The fitting of the experimental data is very good, further indicating that introducing porosity into the matrix can effectively lead the decrease of dielectric constant.

The increase of free volume is mainly brought by the bulky POSS, which can be inferred from the results in Table II. The porosity (in contrast to the dielectric constant) increases with increasing POSS content and decreasing PS arm-length. Simultaneously, it is also found from Table II that the contribution of the intrinsic pore of POSS to the increased free volume is also very small compared with the total increased free volume value, hinting that steric hindrance of bulky POSS plays a dominant role to the increase of free volume and formation of low dielectric constant. If we average ϕ_r^f by POSS content, the relationship between the increase of free volume and PS arm-length is shown in Figure 5. Obviously, increasing the arm-length results in an increase of free volume per POSS content, but this contribution is very small compared with the increase of POSS content. Moreover, it is noticed that PS chains play an important role in preventing the coagulation of POSS in the hybrids.

For further investigating the forming mechanism of dielectric constant of hybrids, the surface tension of the hybrids films was also studied, because the surface tension of materials is affected by the intra/interaction between molecules.[21] Table III shows the static contact angle (Θ) versus the water and glycerol contents, as well as the surface tension or surface free energy (γ_s). The polar (γ_s^p) and dispersive (γ_s^d) components of surface free energy were determined with Wu's harmonic mean method.[37] The static contact angles of water and glycerol for the different PS-POSS hybrid films increase with the increscent POSS content. In the meanwhile, their surface tension (γ_s including γ_s^p and γ_s^d) decreases with increase of POSS content, revealing that introducing bulky POSS into the polymer matrix weakens the intermolecular force of polymeric chains (arms) joined on POSS owing to the increase of the free volume. Obviously, the variation trends of the surface free energy in the POSS-based hybrids are in full accord with that of their dielectric constants, which is also confirmed by Ye's work.[21]

CONCLUSIONS

A series of star-type PS-POSS inorganic–organic hybrids with low dielectric constant were successfully prepared via one-step free-radical polymerization approach, and these hybrids have good film formability and homogeneity. It is found that the low dielectric constants of PS-POSS hybrids is mainly originated from the increased free volume, which is attributed to the steric hindrance of bulky POSS. It is expected that this understanding of the dependence of the low dielectric constant on the structure variation would enlighten the design of new POSS-based hybrid materials with desirable dielectric constant.

ACKNOWLEDGMENTS

This research was financially supported by the National Natural Science Fund of China (Grant Nos. 20971021, 51073031, 21171034 and 20974018), PhD Program Foundation of Ministry of Education of China (No. 20070255012), and National Overseas Scholarship Cooperation Research Foundation of China (No. 50928301).

REFERENCES

1. Lee, W. W.; Ho, P. S. *MRS Bull* **1997,** *22*, 19.
2. Miller, R. D. *Science* **1999,** *286*, 421.
3. Li, Z.; Johnson, M. C.; Sun, M.; Ryan, E. T.; Earl, D. J.; Maichen, W.; Martin, J. I.; Li, S.; Lew, C. M.; Wang, J.; Deem, M. W.; Davis, M. E.; Yan, Y. *Angew Chem. Int. Ed.* **2006,** *45*, 6329.
4. Maex, K.; Baklanov, M. R.; Shamiryan, D.; Iacopi, F.; Brongersma, S. H.; Yanovitskaya, Z. S. *J. Appl. Phys.* **2003,** *93*, 8793.
5. Liu, Y. L.; Liu, C. S.; Cho, C. I.; Hwu, M. J. *Nanotechnology* **2007,** *18*, 225701.
6. Lee, Y. J.; Huang, J. M.; Kuo, S. W.; Chang, F. C. *Polymer* **2005,** *46*, 10056.
7. Tsai, M. H.; Whang, W. T. *Polymer* **2001,** *42*, 4197.
8. Min, C. K.; Wu, T. B.; Yang, W. T.; Chen, C. L. *Compos. Sci. Technol.* **2008,** *68*, 1570.

9. Zhang, Y. H.; Dang, Z. M.; Fu, S. Y.; Xin, J. H.; Deng, J. G.; Wu, J. T.; Yang, S. Y.; Li, L. F.; Yan, Q. *Chem. Phys. Lett.* **2005,** *401*, 553.
10. Wang, H. W.; Shieh, C. F.; Chang, K. C.; Chu, H. C. *J. Appl. Polym. Sci.* **2005,** *97*, 2175.
11. Cordes, D. B.; Lickiss, P. D.; Rataboul, F. *Chem. Rev.* **2010,** *110*, 2081.
12. Leu, C. M.; Reddy, G. M.; Wei, K. H.; Shu, C. F. *Chem. Mater.* **2003,** *15*, 2261.
13. Leu, C. M.; Chang, Y. T.; Wei, K. H. *Chem. Mater.* **2003,** *15*, 3721.
14. Leu, C. M.; Chang, Y. T.; Wei, K. H. *Macromolecules* **2003,** *36*, 9122.
15. Chen, Y. W.; Kang, E. T. *Mater. Lett.* **2004,** *58*, 3716.
16. Chen, Y. W.; Chen, L.; Nie, H. R.; Kang, E. T. *J. Appl. Polym. Sci.* **2006,** *99*, 2226.
17. Wu, S.; Hayakawa, T.; Kikuchi, R.; Grunzinger, S. J.; Kakimoto, M. *Macromolecules* **2007,** *40*, 5698.
18. Wu, S.; Hayakawa, T.; Kakimoto, M.; Oikawa, H. *Macromolecules* **2008,** *41*, 3481.
19. Seckin, T.; Koytepe, S.; Adiguzel, H. I. *Mater. Chem. Phys.* **2008,** *112*, 1040.
20. Chen, W. Y.; Ko, S. H.; Hsieh, T. H.; Chang, F. C.; Wang, Y. Z. *Macromol. Rapid Commun.* **2006,** *27*, 452.
21. Ye, Y. S.; Chen, W. Y.; Wang, Y. Z. *J. Polym. Sci. Polym. Chem.* **2006,** *44*, 5391.
22. Nie, W. Y.; Li, G.; Li, Y.; Xu, H. Y. *Chin. Chem. Lett.* **2009,** *20*, 738.
23. Wahab, M. A.; Mya, K. Y.; He, C. B. *J. Polym. Sci. Polym. Chem.* **2008,** *46*, 5887.
24. Xu, H. Y.; Kuo, S. W.; Lee, J. S.; Chang, F. C. *Polymer* **2002,** *43*, 5117.
25. Xu, H. Y.; Kuo, S. W.; Lee, J. S.; Chang, F. C. *Macromolecules* **2002,** *35*, 8788.
26. Xu, H. Y.; Yang, B. H.; Wang, J. F.; Guang, S. Y.; Li, C. *Macromolecules* **2005,** *38*, 10455.
27. Xu, H. Y.; Yang, B. H.; Wang, J. F.; Guang, S. Y.; Li, C. *J. Polym. Sci. Polym. Chem.* **2007,** *45*, 5308.
28. Lee, L. H.; Chen, W. C. *Polymer* **2005,** *46*, 2163.
29. Yang, B. H.; Xu, H. Y.; Yang, Z. Z.; Liu, X. Y. *J. Mater. Chem.* **2009,** *19*, 9038.
30. Yang, B. H.; Xu, H. Y.; Yang, Z. Z.; Zhang, C. *J. Mater. Chem.* **2010,** *20*, 2469.
31. Zhang, C.; Guang, S. Y.; Zhu, X. B.; Xu, H. Y.; Liu, X. Y.; Jiang, M. H. *J. Phys. Chem. C.* **2010,** *114*, 22455.
32. Richter, A.; Sturm, J. *Appl. Phys. A Mater.* **1995,** *61*, 163.
33. Yang, B. H.; Xu, H. Y.; Wang, J. F.; Gang, S. Y.; Li, C. *J. Appl. Polym. Sci.* **2007,** *106*, 320.
34. Feng, Y.; Jia, Y.; Xu, H. *J. Appl. Polym. Sci.* **2009,** *111*, 2684.
35. Lee, Y. J.; Huang, J. M.; Kuo, S. W.; Lu, J. S.; Chang, F. C. *Polymer* **2005,** *46*, 173.
36. Ye, C.; Ning, Z. *Physics* **2006,** *35*, 322.
37. Wu, S. *J. Polym. Sci. C.* **1971,** *34*, 19.